

# Numerical simulation of sharp crested arced weir

S. Azizi <sup>1</sup>, M. Mehraein <sup>2</sup>

1- Msc student of water and hydraulic structure engineering, Faculty of engineering, Kharazmi University, Tehran, Iran.

2- Assistant Professor, Faculty of engineering, Kharazmi University, Tehran, Iran.

Email: mehraein@khu.ac.ir

## Abstract

Weirs have been used as many shapes in plan; (trapezoid, triangle, arc ....). Nowadays using numerical approaches and ease of access to personal computers and expensive laboratory researches made these approaches reasonable. Arced weir is analyzed in this research numerically. In this research k-ε model were used, this model is one of the widely used model in turbulence simulations. The k-ε model made a good approximation in many types of flows. Higher discharge coefficient is achieved by increasing the length of this type of weir. In this research the results of head and downstream mound are presented using numerical simulation. In all models weir height and vertex angle were 10 cm and 180° respectively. The discharge range was 0.16 to 0.015 m<sup>3</sup>/s. Absolute average errors of total heads over the weir and mound was 3% and 4% percent respectively. Hence, all results indicated a good agreement between numerical simulation and laboratory experiments. Numerical simulation can be used as an appropriate approach to estimate the discharge coefficients of arced weirs.

**Keywords:** Numerical Simulation, Arced Weir, Discharge Coefficients.

## 1. INTRODUCTION

Weirs are used as a part of deviation systems or flood control, by controlling the height of the flow in canals and reservoirs. By increasing the water level in the reservoir, the amount of water that is higher than the top of the weir crest is directed outward. Weirs have different shapes in plan; (triangles, trapezoidal, rectangular, and semicircular). Another category of weirs is based on the type of edges and the height of water on the crown, which is divided into two groups of sharp, broad edges. Based on this classification, if the depth of water on the crown exceeds 5 times the thickness of the crest in the direction of flow, the weir classified as sharp edge [1] & [2]. In this research weir is sharp edge. One of the few studies on arced weirs in the plan was done by Kumar et al. [3]. they introduced arced weirs as a convenient tool for easy and accurate measurement of discharge also they considered the vortex of 90 degrees as the optimum option in arced weirs. Arced shape in other kinds of weirs studied, for example discharge of arced labyrinth weirs as much as twice as classical labyrinth weirs [4].

Another study showed that when weirs inclined in to reservoir, it had twice larger discharge than classical one in channel [5]. Another aspect in weirs that was interested was Discharge efficiency. Discharge efficiency of arc labyrinth weirs were higher than conventional ones located in channels [6]. Variation in discharge coefficient in frontal weirs represented based on Reynolds numbers [7].

Based on researches, if the downstream level of fluid is higher than upstream level, submergence occurred and this phenomenon made less discharge coefficient in weir. According to this subject, an equation for discharge coefficient with respect to submergence ratio was presented [8].

Some researches focused on computing techniques to evaluating hydraulic of labyrinth weirs [9] & [10]. By increasing the length of the arced weir, the discharge increased when other effective parameters were kept constant [11].

The aeration of nape was investigated by some researchers. As the air pressure decreases, the flow curvature increases and the discharge coefficient increase. In this context, Bos, represents an equation for aeration of the weir [12]. The aeration of the arced labyrinth weir better than the normal weirs. (normal weir with equal length) Especially in triangular labyrinth weir by increasing sill slope, aeration will increase [13]. Flow over the weir based on general head-discharge equation could be calculated as below [14]:

$$Q = \frac{2}{3} \times C_d \times L \times (H_T)^{3/2} \times \sqrt{2g} \quad (1)$$

At the above equation,  $H_T$  is total head over the crest of weir,  $g$  is gravity,  $L$  is weir's length and  $C_d$  is discharge coefficient. Flow characteristics and geometry of the weir have effects on  $C_d$  [15]. It can be seen Cleary few investigations have been done on curved weirs so far. The lack of researches on estimating the discharge coefficients of arced weirs and high expense of laboratory tests made us to investigate the numerical simulation of arced weirs.

## 2. AVAILABLE EXPERIMENTAL DATA

The research carried out involves numerical analysis of the flow over the arced weir and its verification using laboratory data. Sangafsi et. al.'s [11] data were used for verification. The reservoir model has two approaches with 10 m length, 2 m width, 0.9 m depth and weir height is 0.10 m (Figure 1). Discharges range was 0.016-0.15 m<sup>3</sup>/s.

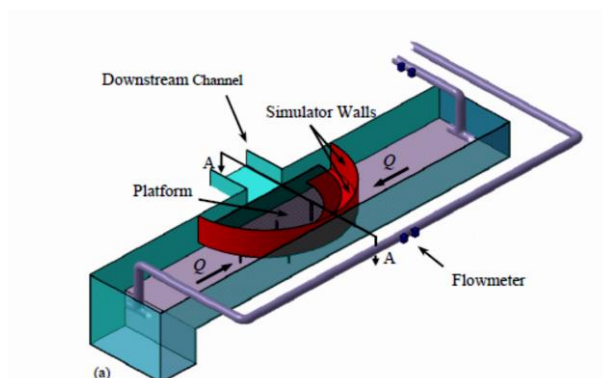


**Figure 1. complete set up of reservoir [7]**

In addition data measurements were done under natural aeration and steady state condition. In this study, two groups of laboratory results were focused first  $H_0/p$  and  $k/p$ . Here,  $H_0$  is the upstream head,  $k$  is the height of downstream mound and  $p$  is the weir height. (figure 2).

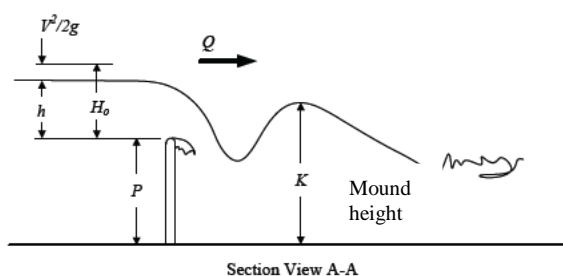


**Figure 2. upstream total head ( $H_0$ ) and downstream mound ( $k$ )**

## 3. NUMERICAL SIMULATION

### 3.1. GOVERNING EQUATION

In this research, FLOW 3D software was used for numerical simulation. This software is widely used today to solve the problems of hydraulic structures. This software is specially developed to solve fluid motion problems. Some of the governing equations are introduced briefly. The mass continuity equations and momentum equations are among the most important of these. The general mass continuity equation is [16]:

$$V_F \frac{\partial \rho}{\partial t} + \frac{\partial}{\partial x} (\rho u A_x) + R \frac{\partial}{\partial y} (\rho v A_y) + \frac{\partial}{\partial z} (\rho w A_z) + \xi \frac{\rho u A_x}{x} = R_{DIF} + R_{SOR} \quad (2)$$

In this equation  $V_f$  is the fractional volume open to flow,  $\rho$  is fluid density,  $R_{DIF}$  is turbulent diffusion term and  $R_{SOR}$  is a mass source. The relations (3), (4) and (5) of the motion equations are about the velocity of the fluid in the directions (u, v, w) and are expressed in three main directions. These relations are the same Navier-Stokes equations with a few variations.

$$\begin{aligned} \frac{\partial u}{\partial t} + \frac{1}{V_F} \left\{ uA_x \frac{\partial u}{\partial x} + vA_y R \frac{\partial u}{\partial y} + wA_z \frac{\partial u}{\partial z} \right\} - \xi \frac{A_y v^2}{xV_F} \\ = -\frac{1}{\rho} \frac{\partial p}{\partial x} + G_x + f_x - b_x - \frac{R_{SOR}}{\rho V_F} (u - u_w - \delta u_s) \end{aligned} \quad (3)$$

$$\begin{aligned} \frac{\partial v}{\partial t} + \frac{1}{V_F} \left\{ uA_x \frac{\partial v}{\partial x} + vA_y R \frac{\partial v}{\partial y} + wA_z \frac{\partial v}{\partial z} \right\} + \xi \frac{A_y v u}{xV_F} \\ = -\frac{1}{\rho} \left( R \frac{\partial p}{\partial y} \right) + G_y + f_y - b_y - \frac{R_{SOR}}{\rho V_F} (v - v_w - \delta v_s) \end{aligned} \quad (4)$$

$$\begin{aligned} \frac{\partial w}{\partial t} + \frac{1}{V_F} \left\{ uA_x \frac{\partial w}{\partial x} + vA_y R \frac{\partial w}{\partial y} + wA_z \frac{\partial w}{\partial z} \right\} \\ = -\frac{1}{\rho} \left( \frac{\partial p}{\partial z} \right) + G_z + f_z - b_z - \frac{R_{SOR}}{\rho V_F} (w - w_w - \delta w_s) \end{aligned} \quad (5)$$

In these equations ( $G_x, G_y, G_z$ ), are the accelerations, ( $f_x, f_y, f_z$ ), are viscous accelerations and ( $b_x, b_y, b_z$ ) are the amount of flow losses in the porous medium or porous plates defined by the user, and finally the last sentence is defined for entering the mass into geometry [16].

### 3.2. TURBULENCE MODEL

A sophisticated and widely used model consists of two transport equations for the turbulent kinetic energy  $k_T$  and its dissipation  $\varepsilon_T$ , the so-called k- $\varepsilon$  model [17] has been used in this paper. An additional transport equations are solved for the turbulent dissipation,  $\varepsilon_T$  and turbulent kinetic energy  $k_T$  [16]:

$$\frac{\partial \varepsilon_T}{\partial t} + \frac{1}{V_F} \left\{ uA_x \frac{\partial \varepsilon_T}{\partial x} + vA_y R \frac{\partial \varepsilon_T}{\partial y} + \omega A_z \frac{\partial \varepsilon_T}{\partial z} \right\} = \frac{CDIS1 \cdot \varepsilon_T}{k_T} (P_T + CDIS3 \times G_T) + DIFF_\varepsilon - CDIS2 \frac{\varepsilon_T^2}{k_T} \quad (6)$$

$$k_T = \frac{1}{2} (\overline{u'^2} + \overline{v'^2} + \overline{w'^2}) \quad (7)$$

Where  $u', v', w'$  are the x, y and z components of the fluid velocity associated with chaotic turbulent fluctuations,  $k_T$  is the specific kinetic energy and u, v, w are the x, y and z components of the fluid velocity,  $DIFF_\varepsilon$  is the diffusion of dissipation,  $V_F, A_x, A_y, A_z$  are FLOW3D's FAVOR functions,  $CDIS1, CDIS2,$  and  $CDIS3$  are all dimensionless user-adjustable parameters,  $G_T$  is The buoyancy production term,  $R$  is related to the cylindrical coordinate system (in this research Cartesian coordinate used) and  $P_T$  is the turbulent kinetic energy production [16]:

$$\begin{aligned} P_T = CSPRO \left( \frac{\mu}{\rho V_F} \right) \left\{ 2A_x \left( \frac{\partial u}{\partial x} \right)^2 + 2A_y \left( R \frac{\partial u}{\partial y} + \xi \frac{u}{x} \right)^2 + 2A_z \left( \frac{\partial w}{\partial z} \right)^2 \right. \\ \left. + \left( \frac{\partial v}{\partial x} + R \frac{\partial u}{\partial y} + \xi \frac{v}{x} \right) \left[ A_x \frac{\partial v}{\partial x} + A_y \left( R \frac{\partial u}{\partial y} - \xi \frac{v}{x} \right) \right] \right. \\ \left. + \left( \frac{\partial u}{\partial z} + \frac{\partial w}{\partial x} \right) \left( A_z \frac{\partial u}{\partial z} + A_x \frac{\partial w}{\partial x} \right) + \left( \frac{\partial v}{\partial z} + R \frac{\partial w}{\partial y} \right) \left( A_z \frac{\partial v}{\partial z} + A_y R \frac{\partial w}{\partial y} \right) \right\} \end{aligned} \quad (8)$$

$CSPRO$  is a turbulence parameter, whose default value is 1.0,  $\mu$  is the molecular dynamic viscosity,  $\rho$  is the fluid density and  $R$  and  $\xi$  are related to the cylindrical coordinate system.

The diffusion of dissipation,  $Diff_\epsilon$ , is [16]:

$$Diff_\epsilon = \frac{1}{V_F} \left\{ \frac{\partial}{\partial x} (v_\epsilon A_x \frac{\partial \epsilon_T}{\partial x}) + \frac{\partial}{\partial y} (v_\epsilon A_y R \frac{\partial \epsilon_T}{\partial y}) + \frac{\partial}{\partial z} (v_\epsilon A_z \frac{\partial \epsilon_T}{\partial z}) + \xi \frac{v_\epsilon A_x \epsilon_T}{x} \right\} \quad (9)$$

### 3.3. NUMERICAL SPECIFICATIONS

The models were created using Auto CAD software and were exported to FLOW 3D. Cartesian coordinate and hexahedral elements were used to represent fluid and solid geometries. Hence, six boundaries have to be defined for each model (figure (4)). In this research time-step was controlled by stability and convergence. In FLOW3D time step calculate automatically (in the range of 0.000025-0.0152 s). Upstream total head was measured at 4p from the crest of the weir to avoid the water surface curvature, [6]. The numerical model specifications are presented at table 1.

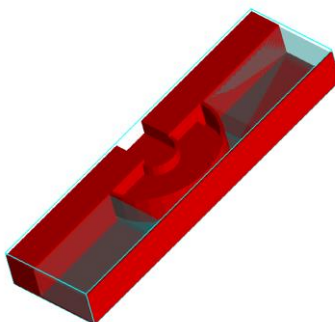


**Figure 3. geometry of the model and initial condition**

The upstream boundary is defined as volume flow rate, downstream end of model is represented as outflow and other boundaries are presented in table 1 and figure 4.

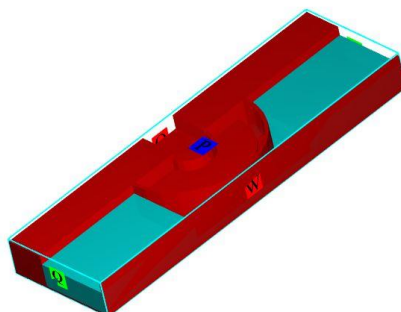


**Figure 4. Boundary conditions**

In figure 4: Q is volume flow rate, W is wall, p is pressure, O is outflow.

**Table 1. meshing and boundary conditions**

<b>mesh</b>	<b>Computational block</b>	<b>1</b>
	<b>Total number of meshes</b>	<b>800000-1000000</b>
<b>Boundary conditions</b>	<b>Downstream</b>	<b>Outflow</b>
	<b>Left boundary</b>	<b>Volume flow rate</b>
	<b>Right boundary</b>	<b>Volume flow rate</b>
	<b>Free surface model</b>	<b>VOF</b>
<b>Equations</b>	<b>Turbulence model</b>	<b>k-ε</b>
	<b>Time interval</b>	<b>0.01</b>

## 4. RESULTS AND VERIFICATION

### 4.1. MOUND HEIGHTS

Figure 5 and 6 show the numerical simulation of water surface profile at the downstream of arced weir. The mound height of the experimental report is also added for comparison (mound configuration illustrated in figure- 2). It is clear, that the crest of the mound simulated with acceptable accuracy.

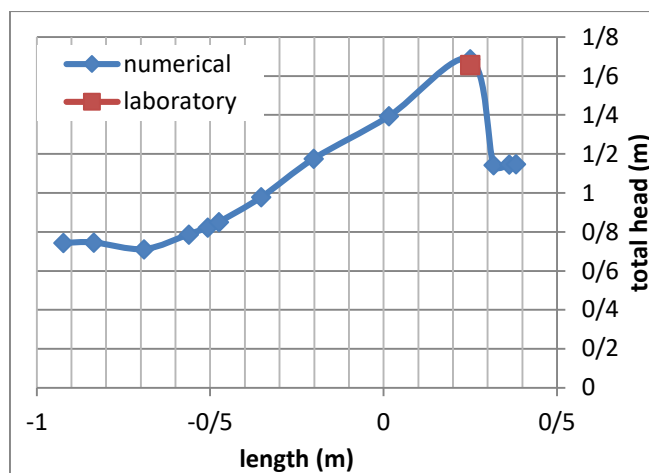


**Figure 5. Numerical & Laboratory mound at Q=0.091 cmfs**

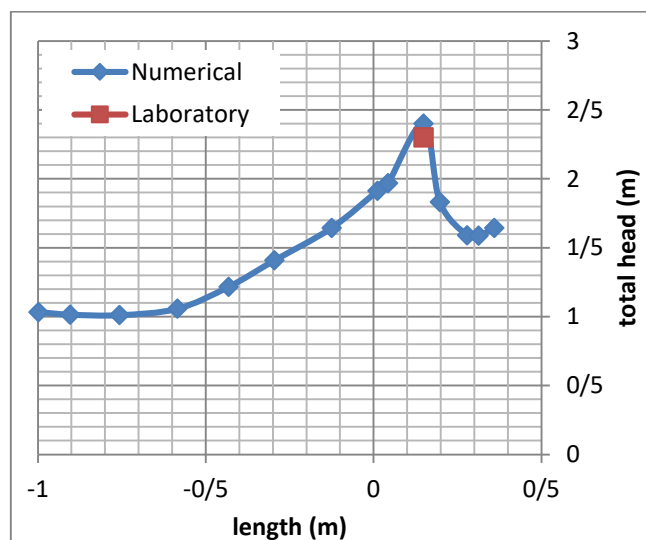


**Figure 6. Numerical & Laboratory mound at Q=0.156 cmfs**

Figure 7 showed simulated and experimental results for the mound height in dimensionless manner. All numerical data have A.A.E (Absolute average error) and RSQ. equal to 4.47 percent and 0.993, respectively. Hence one can concluded that the downstream height of the mound can be simulated numerically with acceptable accuracy. As the mound height has significant effect on discharge coefficient of the weir in the submerged condition, flow- 3D software can be used as an appropriate tool to find the discharge coefficient of the arced weirs.

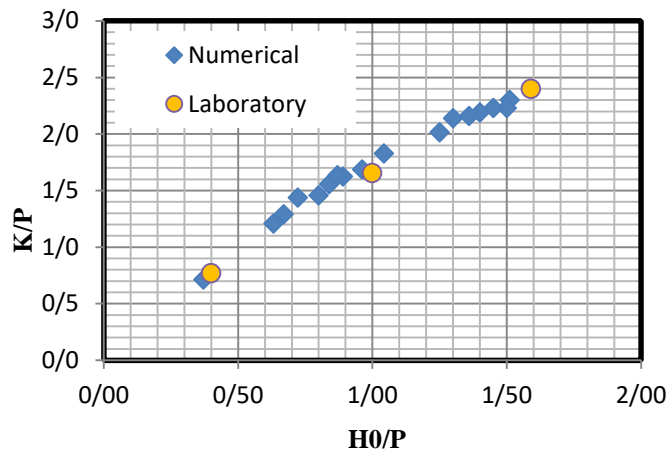


**Figure 7. all results from numerical and laboratory tests**

#### 4.2. UPSTREAM TOTAL FLOW HEAD

Figure (8) showed the total head of of weir for  $Q= 0.091 \text{ m}^3/\text{s}$ . The error of the numerical simulation is 3%.

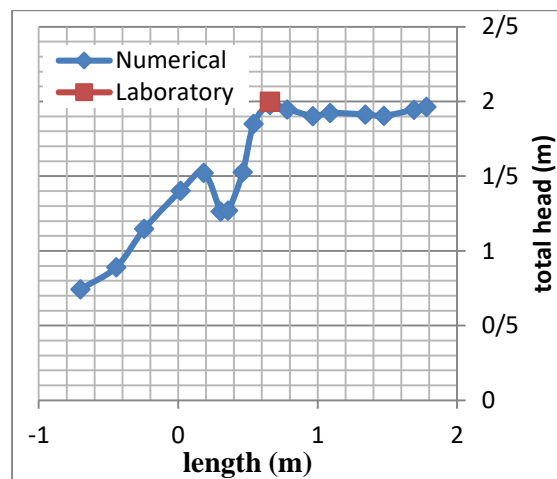


**Figure 8. Total head against length (all dimension in meter)**

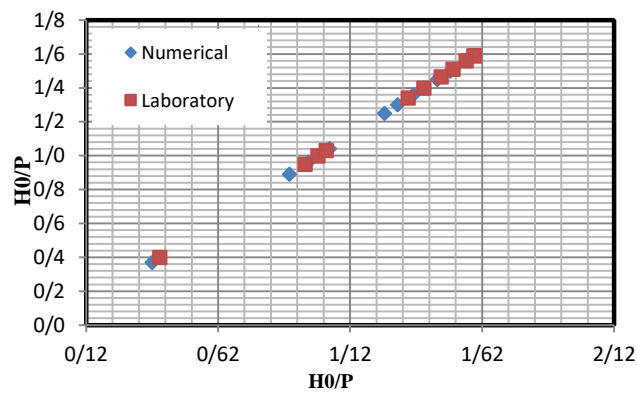


**Figure 9. comparing between upstream heads of numerical simulation and laboratory tests**

It should be mention that for all numerical simulation, A.A.E (absolute average error) is less than 3 % (Figure 9).

## 5. CONCLUSIONS

Arched weirs could be used as measuring device. In numerical simulation all results indicated that mound height had less than 5% differences from laboratory runs and total upstream head had 3% error. Finally by comparing results between laboratory and numerical simulation, good agreement was seen and because of time consuming and higher price of laboratory runs, we suggest that numerical simulation could be the sufficient substitution.

## 6. REFERENCES

1. Vischer, D; “*Recent developments in spillway design*”. Journal of Water Power and Dam Construction, Vol.40, No. 1, 1988, pp: 10-15.
2. Hanger, W. H; and Schwalt, “*Broad-crested weir*”. American Society of Civil Engineering, Journal of the Hydraulics Division, Vol. 120, No. 2, 1994, pp:13-27.
3. Kumar S., Ahmad Z., Mansoor T. and Himanshu S.K. (2012),“*Discharge Characteristics of Sharp Crested Weir of Curved Plan-form,*”Research Journal of Engineering Sciences ISSN 2278 – 9472 Vol. 1(4), pp: 16-20.
4. Yildiz, D. and Uzecek, E. (1996). “*Modeling the performance of labyrinth spillways*” Hydropower & Dams. Aqua-Media Int. Ltd., Surrey, UK. 3:71-76.
5. Houston, K. (1983). “*Hydraulic model study of Hyrum Dam auxiliary labyrinth spillway*” U.S. Bureau of Reclamations, Denver, Colo., # GR 82-13, pp: 9-10.
6. Crookston, B. M; and Tullis, B. P (2012). “*Discharge Efficiency of Reservoir-Application-Specific Labyrinth Weirs*”. ASCE , Vol. 138, No. 6, pp: 564-568.
7. Aydin, I. “*Flow Measurement and Instruction*”. Journal of Hydraulic Research, 2011, pp: 144-151.
8. Villemonte J. R; “*Submerged weir discharge studies*”. Engineering News Record, Vol. 139, No. 26, 1947, pp: 54-56.
9. Emiroglu M.E., Kisi O. and Bilhan O. (2010), “*Predicting discharge capacity of triangular labyrinth side weir located on a straight channel by using an adaptive neurofuzzy technique,*” Adv Eng Softw, 41(2), pp: 54–160.
10. Bilhan O., Emiroglu M.E. and Kisi O. (2010), “*Application of two different neural network techniques to lateral outflow over rectangular side weirs located on a straight channel,*” Adv Eng Softw., 41(6), 831–7.
11. Sangsefidi Y., Mehraein M., Ghodsian M. and Motalebizadeh M. (2017) “*Evaluation and analysis of flow over arched weirs using traditional and response surface methodologies,*” J. Hydraul. Eng., (Accepted for publication).
12. Bos, M. G (1976) “*Discharge measurement structures*”. International Institute For Land Reclamation and Improvement, Wageningen, the Netherlands,.
13. Emiroglu M.E. and Baylar A. (2005), “*Influence of included angle and sill slope on air entrainment of triangular planform labyrinth weirs,*” ASCE J Hyd Eng; 131(3),pp: 184–9
14. Henderson, F. (1966). “*Channel controls*”Open channel flow. MacMillan, New York, 174-176.
15. Bagheri S. and Heidarpour M. (2010), “*Application of free vortex theory to estimate discharge coefficient for sharp-crested weirs,*” Biosystems Engg., 105 (3), 423–7.
16. Flow-3D, User Manual Version 11.2, Flow Science, Inc., Santa Fe (2016).
17. Francis H. Harlow and P. I. Nakayama. (1967) “*Turbulence transport equations,*” Physics of Fluids, 10(11):2323–2332.
18. Rodi. W. (1980) “*Turbulence models and their application in hydraulics: a state of the art review.*” International Association for Hydraulic Research (IAHR), Delft, The Netherlands.